

Organic & Biomolecular Chemistry

Accepted Manuscript



This is an *Accepted Manuscript*, which has been through the Royal Society of Chemistry peer review process and has been accepted for publication.

Accepted Manuscripts are published online shortly after acceptance, before technical editing, formatting and proof reading. Using this free service, authors can make their results available to the community, in citable form, before we publish the edited article. We will replace this *Accepted Manuscript* with the edited and formatted *Advance Article* as soon as it is available.

You can find more information about *Accepted Manuscripts* in the [Information for Authors](#).

Please note that technical editing may introduce minor changes to the text and/or graphics, which may alter content. The journal's standard [Terms & Conditions](#) and the [Ethical guidelines](#) still apply. In no event shall the Royal Society of Chemistry be held responsible for any errors or omissions in this *Accepted Manuscript* or any consequences arising from the use of any information it contains.

ARTICLE

Tri- and tetra-substituted cyclen based lanthanide(III) ion complexes as ribonuclease mimics: A study into the effect of $\log K_a$, hydration and hydrophobicity on phosphodiester hydrolysis of the RNA-model 2-hydroxypropyl-4-nitrophenyl phosphate (HPNP)

Cite this: DOI: 10.1039/x0xx00000x

Received 00th January 2012,
Accepted 00th January 2012

DOI: 10.1039/x0xx00000x

www.rsc.org/

Ann-Marie Fanning,^a Sally. E. Plush^{b*} and Thorfinnur Gunnlaugsson^{a*}

A series of tetra-substituted 'pseudo' dipeptide ligands of cyclen (1,4,7,10-tetraazacyclododecane) and a tri-substituted 3'-pyridine ligand of cyclen, and the corresponding lanthanide(III) complexes were synthesised and characterised as metallo-ribonuclease mimics. All complexes were shown to promote hydrolysis of the phosphodiester bond of 2-hydroxypropyl-4-nitrophenyl phosphate (HPNP, $\tau_{1/2} = 5.87 \times 10^3$ h), a well known RNA mimic.¹ The La(III) and Eu(III) tri-substituted 3'-pyridine lanthanide(III) complexes being the most efficient in promoting such hydrolysis at pH 7.4 and at 37 °C; with $\tau_{1/2} = 1.67$ h for La(III) and 1.74 h for Eu(III). The series was developed to provide the opportunity to investigate the consequences of altering the lanthanide(III) ion, coordination ability and hydrophobicity of a metallo-cavity on the rate of hydrolysis using the model phosphodiester, HPNP, at 37 °C. To further provide information on the role that the $\log K_a$ of the metal bound water plays in phosphodiester hydrolysis the protonation constants and the metal ion stability constants of both a tri and tetra-substituted 3'-pyridine complex were determined. Our results highlighted several key features for the design of lanthanide(III) ribonuclease mimics; the presence of two metal bound water molecules are vital for pH dependent rate constants for Eu(III) complexes, optimal pH activity approximating physiological pH (~7.4) may be achieved if the $\log K_a$ values for both MLOH and ML(OH)₂ species occur in this region, small changes to hydrophobicity within the metallo cavity influence the rate of hydrolysis greatly and an amide adjacent to the metal ion capable of forming hydrogen bonds with the substrate is required for achieving fast hydrolysis.

Introduction

The phosphodiester bond¹ is fundamental to many biological systems as it forms the stable backbone of DNA and RNA and as such is vital for the encoding of genetic information.^{2, 3} The remarkable hydrolytic stability of this bond is important for the prevention of accidental DNA corruption and the preservation of genetic codes.⁴ Nevertheless, the sequence-specific hydrolytic cleavage of DNA and RNA is important not only in metabolic and regulatory processes but also in the fields of molecular biology, biochemistry and most importantly in the development of novel cancer therapies.⁵

Over the last 20 years much interest has focused on the rational design of hydrolytic enzyme mimics⁶⁻¹¹ which can provide mechanistic insight into the chemical process of hydrolysis, be employed as artificial restriction enzymes for molecular biology and

help realise the development of anti-DNA drugs in the near future.¹² Effective examples of hydrolytic enzyme mimics exist based on both transition metals (Zn(II), Fe(III), etc) and the lanthanide(III) series.¹³⁻¹⁸ Many of these examples have been developed by Morrow and co-workers who have made significant discoveries in this arena (only a few select references of this extensive work are cited here).¹⁹⁻²¹ The lanthanide(III) ion series possess very attractive properties for hydrolytic cleavage, especially when compared with the transition metals, notably the absence of accessible redox chemistry, strong Lewis acidity, high coordination numbers and charge density and fast ligand-exchange rates.²² The latter is very favourable from a reactant binding and product release viewpoint. To this end a variety of lanthanide(III) ion complexes have been prepared by us^{16, 23} and others.^{15, 24-27} The design of which has been dominated by the properties of the metal ion, ligand structure, hydrophobicity of the system and ultimately the $\log K_a(s)$ of the associated metal bound

water(s). However, there is still a demand for the further systematic study of the effect of structural changes on the hydrolytic ability of the complex.

Some of the most efficient single lanthanide(III) ion complexes for phosphodiester hydrolysis have been developed by us; one of the earliest examples from this group showed that the introduction of pseudo dipeptides, such as 'GlyGly', **1.Ln(III)**, and 'GlyAla', **2.Ln(III)**, into the cyclen framework (Figure 1) substantially increased the rate of phosphodiester hydrolysis compared with the uncatalysed reaction. For example **1.Ln(III)** was found to cleave HPNP with a pseudo first order rate constant of 0.41 h^{-1} and $\tau_{1/2}$ of 1.7 h at pH 7.4 and 37°C .[†] This is a 3400-fold rate enhancement over the un-catalysed reaction.^{1, 28} It is postulated that the deep bowl shaped cavity adopted by the pendant donor arms upon lanthanide(III) ion complexation, as confirmed by X-ray crystallography for **2.Ln(III)**,²⁹ plays an important role by creating a hydrophobic environment. Increased hydrophobicity is believed to facilitate the formation of stronger interactions between the metal ion and the substrate, further aiding phosphodiester hydrolysis.^{29, 30}

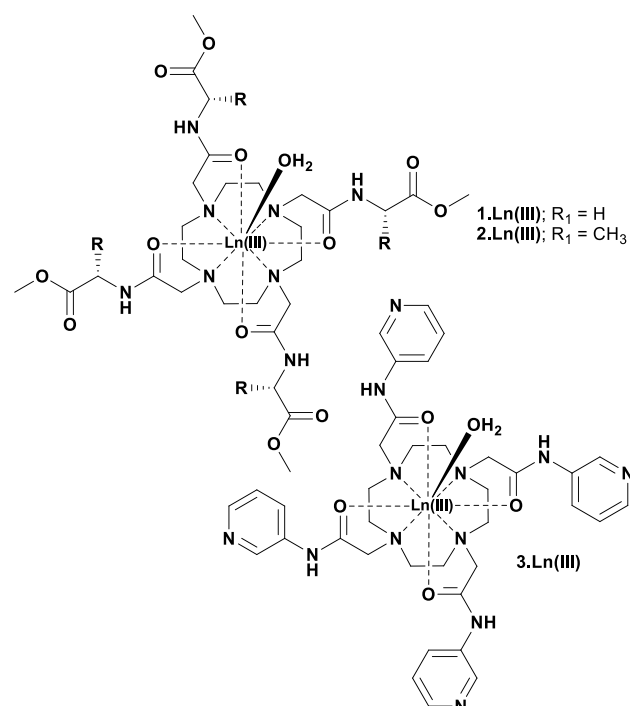


Fig. 1 Schematic representation of previously reported complexes for phosphodiester hydrolysis (**1.Ln(III)**, **2.Ln(III)** and **3.Ln(III)**).

One of the most efficient examples of HPNP hydrolysis from our work is the tetra-substituted 3'-pyridine cyclen complex, **3.Ln(III)**, Figure 1. Complex **3.La(III)** was found to promote hydrolysis of HPNP with a k of $0.440 (\pm 0.014) \text{ h}^{-1}$ and a $\tau_{1/2} \sim 1.6 \text{ h}$. This rate constant represents a 3666-fold rate increase over the un-catalysed reaction.³¹ It is postulated that in addition to forming a concave metal ion induced cavity structure, the 3'-pyridine groups also promote acid-base catalysis by 'tuning' the $\log K_a$ of the metal bound water. Furthermore, it is believed that the nitrogen's of the pyridine rings hydrogen bond to the substrate helping to stabilise the transition state. All of which combine to promote phosphodiester hydrolysis. Therefore, in continuation of our ongoing research in understanding the effect of pendant arms or 'co-factors' and the role of the metal bound water on the rate of hydrolysis of phosphodiester bonds, we have synthesised four new

lanthanide(III) ion macrocyclic complexes, as shown in Scheme 1; a tri-substituted 3'-pyridine complex, **4.Ln(III)**, and three 'pseudo' dipeptide tetra substituted complexes, **5.Ln(III)**, **6.Ln(III)** and **7.Ln(III)**.

It was anticipated that the tri-substituted cyclen complex, **4.Ln(III)**, would be more efficient towards hydrolysis, compared with the previously reported tetra-substituted **3.Ln(III)** complex. The use of only three pendant arms is predicted to result in an increase in the number of metal bound water molecules (three in the case of La(III) and two for Eu(III)) and an increase in the number of coordination sites available. The latter may be advantageous for substrate binding. The number of metal bound water molecules will be calculated by measuring the lifetime of each complex in both H_2O and D_2O and using the revised Horrocks equation to determine the q value.^{32, 33} The three 'pseudo' dipeptide tetra substituted complexes, **5.Ln(III)**, **6.Ln(III)** and **7.Ln(III)**, were designed to further explore how the nature of the hydrophobic cavity formed around the metal ion influences hydrolysis of HPNP. This may potentially provide information on the mechanism of RNA cleavage, which as yet is not universally defined.^{34, 35} It was hypothesised that *N*-methylation of the previously reported pseudo 'GlyGly dipeptide' amide, **1.Ln(III)**,²⁸ to generate **5.Ln(III)** would further increase hydrophobicity in the cavity which may in turn increase activity. *N*-Methylation is used to improve *in vivo* stability in medicinal chemistry. It was also proposed that by introducing amino amide arms (**6.Ln(III)** and **7.Ln(III)**) in place of the previously reported amino ester arms present in **1.Ln(III)**²⁸ and **2.Ln(III)**²⁹ would increase hydrogen bonding to the phosphodiester backbone and/or the outer sphere water molecules and that this in turn would increase the rate of hydrolysis.³⁶ Furthermore, the decreased steric bulk of the amide compared with the ester group was expected to facilitate substrate access to the metal ion. In addition it was also anticipated that the pseudo 'dipeptide' amino amide arms would show increased water solubility, hence making the hydrolytic agents more suitable for *in vivo* applications. Information on how changing hydrophobicity of the cavity at varying distances from the metal ion affects the rate of hydrolysis will be generated by comparing the rates of hydrolysis between the three dipeptides, **5.Ln(III)**, **6.Ln(III)** and **7.Ln(III)**. This is important for the generation of future RNA hydrolysis mimics.

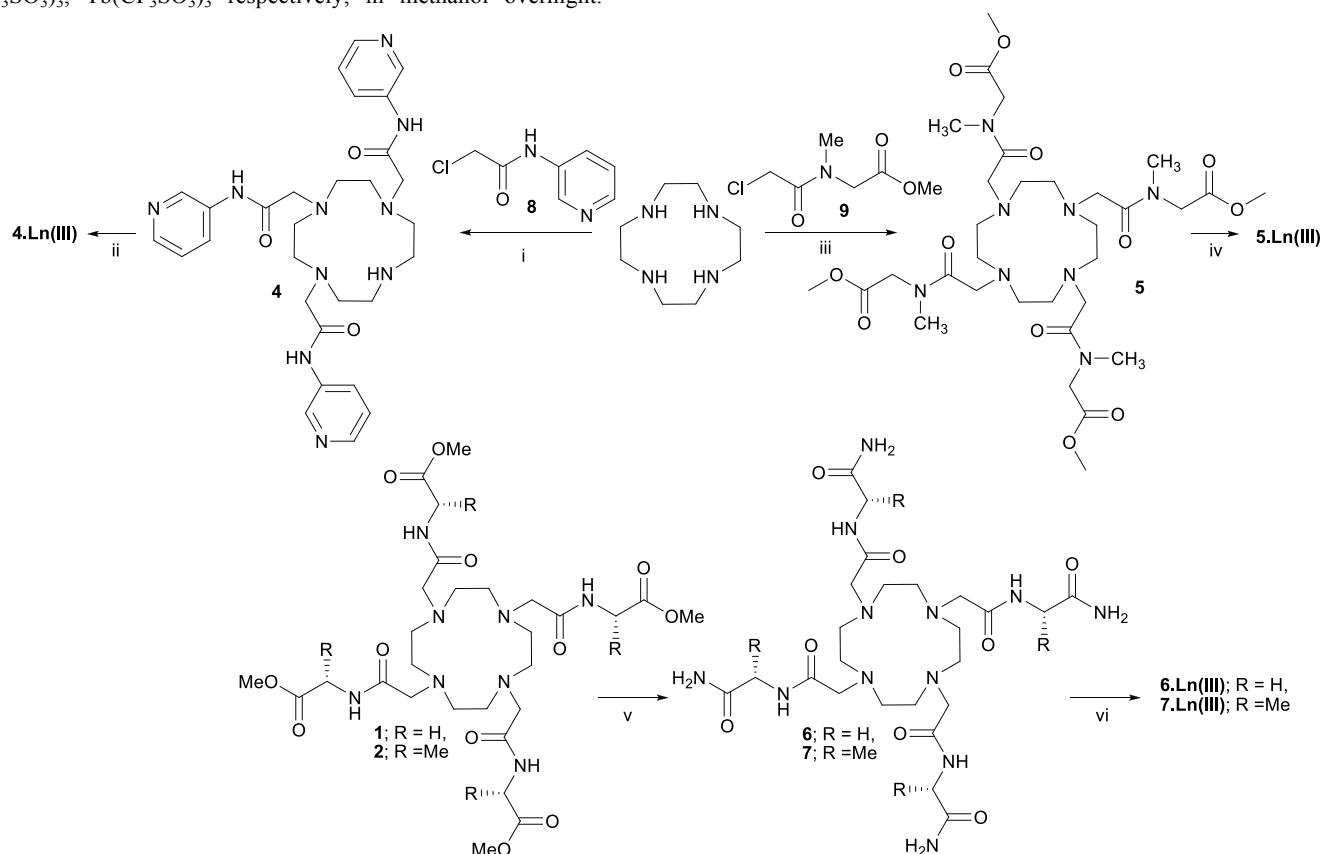
Results and discussion

Synthesis of ligands 4, 5, 6 and 7 and their corresponding La(III), Tb(III) and Eu(III) complexes

A schematic diagram for the synthesis of the tri-substituted ligand, **4**, and the corresponding lanthanide(III) ion complexes, **4.Ln(III)**, are shown in Scheme 1. Preparation of the chloroacetamide 3'-amino pyridine pendant arm, **8**, was achieved by reacting 3'-amino pyridine with chloroacetyl chloride in acetone at -20°C in the absence of base. The product was obtained as an HCl salt following filtration. Characterisation of this compound showed that no further purification was required. Three molar equivalents of this α -chloro acetamide, **8**, were then reacted with cyclen in the presence of Cs_2CO_3 and catalytic quantities of KI in methanol at 65°C for 4 days. The inorganic salts were then removed by filtration and the tri-substituted ligand, **4**, obtained as a cream solid in 38% yield following alumina column chromatography. The $^{13}\text{C}\{^1\text{H}\}$ decoupled NMR spectra (ESI Figure S1) clearly reflects the C_2 symmetry of the molecule; 10 resonances can be observed from the pyridine moieties, indicating that the carbons of the pyridine ring are not all equal and that a tri-substituted system had formed.

The lanthanide(III) ion complexes **4.La(III)**, **4.Eu(III)** and **4.Tb(III)** were formed by heating **4** at reflux with $\text{La}(\text{CF}_3\text{SO}_3)_3$,

Eu(CF₃SO₃)₃, Tb(CF₃SO₃)₃ respectively, in methanol overnight.



Scheme 1. Structures of the tri-substituted 3-pyridine complex (**4.Ln(III)**) and the tetrasubstituted pseudo dipeptide complexes (**5.Ln(III)**, **6.Ln(III)** and **7.Ln(III)**); Ln(III) = La(III), Eu(III) or Tb(III). Reagents and conditions: (i) Cs₂CO₃, KI, MeOH, 65 °C, 72 h, ligand **4**: 36% yield; (ii) Ln(CF₃SO₃)₃, MeOH, 16 h, **4.La(III)**: 86% yield, **4.Eu(III)**: 80% yield, **4.Tb(III)**: 87% yield; (iii) Cs₂CO₃, KI, MeCN, 65 °C, 72 h, ligand **5**: 75% yield; (iv) Ln(CF₃SO₃)₃, MeOH, 16 h, **5.La(III)**: 91% yield, **5.Eu(III)**: 82% yield; (v) NH₃, MeOH, 0 °C 1 h, rt 12 h, ligand **6**: 91% yield, ligand **7**: 93% yield; (vi) Ln(CF₃SO₃)₃, MeOH, 16 h, **6.La(III)**: 79% yield, **6.Eu(III)**: 63% yield, **7.La(III)**: 47% yield, **7.Eu(III)**: 78% yield.

Following precipitation and filtration the desired complexes were obtained as pale yellow hygroscopic solids with yields ranging from 80–87%.

The ¹H NMR spectra of **4.Eu(III)** and **4.Tb(III)** showed the presence of the paramagnetic metal ion centres, as indicated by several broad resonances appearing over a large ppm range. For example, the ¹H NMR of **4.Eu(III)** has resonances appearing at 19.07, 9.39, 8.25, 7.06, 6.62, 3.40, 2.87, 1.04, –6.43, –7.69, –10.49, –14.90, –18.48, –19.19 ppm. The upper and lower field chemical shift values of the macrocyclic ring (axial and equatorial protons) indicate that the predominant isomer is square antiprismatic.³⁷ The occurrence of a small signal between 10–25 ppm in the ¹H NMR spectra does suggest that the twisted square antiprismatic isomer is also present in small quantities and is expected to be in equilibrium with the major square antiprismatic isomer.³⁸

Ligand **4** only provides seven donor atoms for complexation, therefore it was expected that both the Eu(III) and Tb(III) complexes would possess two metal bound water molecules while the La(III) complex would possess three metal bound water molecules. The coordination environment of each of the complexes was confirmed either through elemental analysis or by determining the *q* value. The *q* value was determined by measuring the lifetime of each complex in both H₂O and D₂O using the revised Horrock's equation.^{32, 33} As already stated this increase in hydration and available substrate coordination sites is anticipated to alter the rate of phosphodiester hydrolysis. The *q* value for **4.Eu(III)** was found to be 2.0 further

confirming that **4.Eu(III)** possess two metal bound water molecules (Table 1).

Table 1 Lifetime studies for **4.Eu(III)** and **4.Tb(III)** complexes

Complex	H ₂ O		D ₂ O		<i>q</i> = ±0.5
	<i>k</i> (ms ⁻¹)*	<i>τ</i> (ms)*	<i>k</i> (ms ⁻¹)*	<i>τ</i> (ms)*	
4.Eu(III)	3.902	0.256	1.670	0.599	2.04
4.Tb(III)	0.887	1.127	0.440	2.271	1.94

* *k* and *τ* values are quoted with a ± 10% error

A *q* value of ~2.0 was also obtained for **4.Tb(III)** indicating that Tb(III) and Eu(III) have similar coordination environments. These hydration states were also seen using elemental analysis of **4.La(III)** and **4.Eu(III)**, where both showed the presence of the appropriate number of metal bound water molecules.

Elemental analysis on samples that were dried under high vacuum for 16 hour prior to use was performed in duplicate on separate samples to ensure reproducibility of these results. The synthesis of the tertiary amide based ligand system, **5**, was achieved by reacting sacrosine methyl ester with chloroacetyl chloride to generate the α-chloro acetamide pendant arm, **9** in 54 % yield. This was then reacted with cyclen to generate the tetra substituted ligand, **5**. The identification of **5** by NMR spectroscopy proved difficult due to the presence of the tertiary amide of the pendent donor arm. Tertiary amides exhibit slow rotation about the C-N bond at room temperature and have high barriers to rotation. As a result of this a poor ¹H NMR spectrum is observed with broad signals.³⁹ This can

be overcome by using high temperature experiments, which speeds up rotation and averages out the two structures which result from slow bond rotation.³⁹ The ¹H NMR of ligand **5** was recorded at 50 °C in order to fully elucidate the structure of the ligands. This ligand was then heated at reflux with 1.1 equivalents of either La(CF₃SO₃)₃ or Eu(CF₃SO₃)₃ in dry acetonitrile followed by precipitation from diethyl ether to yield **5.La(III)** and **5.Eu(III)**, respectively. These complexes were purified in the same manner as those discussed above and were characterised by ESMS, HRMS, IR and NMR spectroscopy.

Formation of the pseudo amino amide dipeptide complexes, **6.Ln(III)** and **7.Ln(III)**, was achieved by converting the previously reported tetra-substituted glycine or L-alanine methyl ester ligands **1**²⁸ and **2**²⁹, respectively, to the corresponding amides, **6** and **7** respectively (Scheme 1). This was achieved by dissolving ligands **1** and **2** in methanol and saturating the solution with anhydrous ammonia at 0°C for 1 hour, followed by stirring at room temperature for 12 hours. The solvent volume was then reduced and filtered to yield the pseudo amino amide dipeptide ligands **6** and **7** in 91 % and 98% yields, respectively. The cyclen protons and carbons of both **6** (ESI Figure S2) and **7** appeared as single resonances in both the ¹H and ¹³C{¹H} NMR spectra, thus confirming the C₄ symmetry of each ligand.

The lanthanide(III) ion complexes **6.La(III)**, **6.Eu(III)**, **7.La(III)** and **7.Eu(III)** were formed by heating either **6** or **7** at reflux with either La(CF₃SO₃)₃ or Eu(CF₃SO₃)₃ to yield water soluble complexes in varying yields. As expected the introduction of amino amide arms into the pseudo dipeptide structure increased the overall water solubility of these complexes. This is highly desirable for *in vivo* applications. The ¹H NMR spectra for both **6.Eu(III)** (ESI Figure S3) and **7.Eu(III)** showed several broad resonances appearing over a large ppm range, this is consistent with the effect of the paramagnetic ion. The involvement of the pendant donor arms in the coordination complex was confirmed by IR spectroscopy. The single carbonyl stretching frequency occurring at 1662 cm⁻¹ in ligand **6** was shifted when complexed to La(III), or Eu(III) to 1632 cm⁻¹ or 1630 cm⁻¹, respectively, an indication that the pendant donor arms were bound to the metal ion centre. Complexes **7.La(III)** and **7.Eu(III)** were characterised in a similar manner to **6.Ln(III)**.

Protonation constants (logK_a) and metal complex ion formation constants (logK) values

One of the advantages of using cyclic ligands for the formation of lanthanide(III) complexes, is that they can influence the Lewis acidity of metal ions and hence the logK_a of the metal bound water molecules. This can have an effect on metal ion promoted phosphodiester hydrolysis, as the metal bound hydroxide can be of assistance in promoting phosphodiester hydrolysis.⁴⁰ Determination of logK_a values of the metal bound water molecules are known to give insight into the mechanism and reveal important information about pH dependence for complexes which contain pendant donor arms with protonatable groups. Protonation and metal complex stability constants have been investigated for both the previously reported tetra substituted 3'pyridine ligand, **3**, and the tri substituted 3'pyridine ligand, **4**, with the aim of giving insight into the differences lanthanide(III) ion and coordination ability have on the overall stability of the lanthanide(III) complex and the logK_a(s) of the metal bound water molecules.

The protonation constants for the protonated ligand **3** and **4** were determined in H₂O (with constant ionic strength, I = 0.1 M (NEt₄ClO₄)) by potentiometric titration. All solutions were acidified to ensure complete protonation of all basic nitrogen donor atoms. These protonated ligands were then deprotonated gradually by the

titration of NEt₄OH. The protonation constants determined for ligands **3** and **4** are given in Table 2. Potentiometric titration of ligands **3** and **4** showed that the steric bulk of the 3'-pyridine pendant arms increased the hydrophobicity of the macrocyclic ring amines as compared with cyclen (logK_{a1-4} 10.38, 9.71, 2.05, <1).⁴¹ Hydrophobicity decreases the solvation of the amine group, which decreases acidity; increasing hydrophobicity is expected to result in increased hydrolytic efficiency.

The calculation of the metal complex ion formation constants for the metal ion complex ions of La(III) and Eu(III) with **3** and **4** were achieved by means of the computer program HYPERQUAD.⁴² The pH range of the titrations for the determination of the metal complex ion formation constants was limited due to the formation of hydroxide species. The titration curve of the protonated ligand **4**, in the absence and presence of La(ClO₄)₃ and Eu(ClO₄)₃ against NEt₄OH are represented in Figure 2 (the titration curve of the protonated ligand **3**, in the absence and presence of La(ClO₄)₃ and Eu(ClO₄)₃ against NEt₄OH can be seen in the ESI Figure S4 for **3**). In solution, the metal competes with the protons in the acidic media for ligand coordination sites, altering the pH of the solution. Therefore, a change in the titration curve on addition of metal ion to the solution indicates the formation of a metal complex ion; the larger the change, the higher the metal complex ion formation constant. From Figure 2, a significant difference in the titration curve for ligand **4** in the absence and presence of Eu(III) ions at an early pH value is evident. The same can be noted for ligand **3** in the absence and presence of Eu(III) ions (ESI Figure S4). This suggests that both ligands **3** and **4** form quite stable complexes with Eu(III) ions. The formation constants for the formation of the ML species (where M = metal ion, L = ligand) for both ligands **3** and **4** can be seen in Table 2.

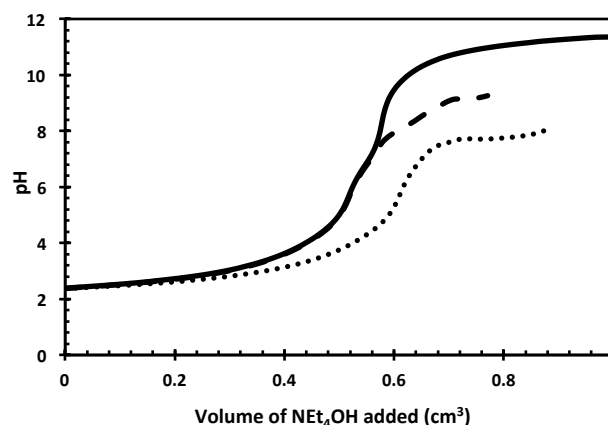


Fig. 2 Titration curves of the protonated ligand **4**, in the absence and presence of La(ClO₄)₃ and Eu(ClO₄)₃ against NEt₄OH at 25 °C. [**4**]_{total} = 7.2 × 10⁻⁴ M (bold line), [La(III)]_{total} (dash line) or, [Eu(III)]_{total} (dotted line) = 7.0 × 10⁻⁴ M, [H⁺]_{total} = 6.4 × 10⁻³ M, [NEt₄OH] = 0.103 M, I = 0.10 M (NEt₄ClO₄), total volume = 10 cm³.

From Table 2, it can be seen that the Eu(III) ions form a more stable ML complex with the tri-substituted ligand **4** compared with the tetra-substituted ligand **3**. This suggests that there is a good match between the high degree of flexibility within the tri-substituted species, **4**, with the size and high surface charge density of the Eu(III) ion, thus favouring stronger binding and higher stability constants. The formation constants of the ML complexes presented herein are lower than comparable DOTA and DO3A complexes.⁴³ The DOTA and DO3A complexes contain carboxylic acid pendant arms which at low pH are negatively charged and thus form favourable interactions with the positively charged lanthanide ions. In contrast in the two 3'pyridine systems presented herein, **3**

and **4**. However, in contrast to the DOTA and DO3A systems, where the tetra-substituted species

Table 2. Stepwise protonation constants and formation constants for **3** and **4** obtained at 25 °C with $I = 0.1$ M (NEt_4ClO_4) in H_2O in the absence and presence of Eu(III) .

Stepwise protonation constants ($\log K_a$)	Stability constants ($\log K$)		3.Eu(III)^a	4.Eu(III)^b	
	3^a	4^b			LogK
$\log K_{a1}$	9.26 ± 0.01	9.39 ± 0.03	$\text{Eu}^{3+} + \text{L} \rightleftharpoons [\text{Eu(L)}]^{3+}$	16.49 ± 0.02	18.56 ± 0.05
$\log K_{a2}$	6.71 ± 0.03	5.82 ± 0.01	$\text{Eu}^{3+} + \text{HL}^+ \rightleftharpoons [\text{Eu(HL)}]^{4+}$	12.19 ± 0.05	9.53 ± 0.05
$\log K_{a3}$	4.51 ± 0.05	4.19 ± 0.02	$\text{Eu}^{3+} + \text{H}_2\text{L}^{2+} \rightleftharpoons [\text{Eu(H}_2\text{L)}]^{5+}$	8.32 ± 0.05	6.09 ± 0.04
$\log K_{a4}$	3.79 ± 0.02	3.30 ± 0.01	$\text{Eu}^{3+} + \text{H}_3\text{L}^{2+} \rightleftharpoons [\text{Eu(H}_3\text{L)}]^{6+}$	6.54 ± 0.05	4.13 ± 0.03
$\log K_{a5}$	3.06 ± 0.05	3.11 ± 0.09	$\text{Eu}^{3+} + \text{H}_4\text{L}^{2+} \rightleftharpoons [\text{Eu(H}_4\text{L)}]^{7+}$	5.61 ± 0.05	-
$\log K_{a6}$	2.53 ± 0.03	low	logK_a		
$\log K_{a7}$	low	low	$[\text{Eu(HL)}]^{4+} \rightleftharpoons [\text{Eu(L)}]^{3+} + \text{H}^+$	6.85 ± 0.04	4.82 ± 0.06
$\log K_{a8}$	low	-	$[\text{Eu(H}_2\text{L)}]^{5+} \rightleftharpoons [\text{Eu(HL)}]^{4+} + \text{H}^+$	4.59 ± 0.19	3.72 ± 0.07
			$[\text{Eu(H}_3\text{L)}]^{6+} \rightleftharpoons [\text{Eu(H}_2\text{L)}]^{5+} + \text{H}^+$	3.71 ± 0.07	2.84 ± 0.04
			$[\text{Eu(H}_4\text{L)}]^{7+} \rightleftharpoons [\text{Eu(H}_3\text{L)}]^{6+} + \text{H}^+$	2.95 ± 0.15	-
			$\text{EuL}^{3+} \rightleftharpoons [\text{EuL(OH)}]^{2+} + \text{H}^+$	7.43 ± 0.01	7.39 ± 0.06
			$[\text{EuL(OH)}]^{2+} \rightleftharpoons [\text{EuL(OH)}_2]^{+} + \text{H}^+$	-	7.90 ± 0.05

^a $[\mathbf{3}] = 9.4 \times 10^{-4}$ M, $[\text{H}^+] = 8.17 \times 10^{-3}$ M, $[\text{NEt}_4\text{OH}] = 0.103$ M, $[\text{Eu(III)}]_{\text{total}} = 1.0 \times 10^{-3}$ M. ^b $[\mathbf{4}] = 7.2 \times 10^{-4}$ M, $[\text{H}^+] = 6.4 \times 10^{-3}$ M, $[\text{NEt}_4\text{OH}] = 0.103$ M, $[\text{Eu(III)}]_{\text{total}} = 7.0 \times 10^{-4}$ M.

exhibits the higher stability, for the 3'pyridine systems, the tri-substituted species exhibits the higher stability. This observation can be explained by again considering the presence of the 3'pyridine groups. The tetra-substituted 3'pyridine ligand, **3**, will be more positively charged at low pH compared with the tri-substituted 3'pyridine ligand, **4**. Hence, it is not unexpected that the tri-substituted species forms a more favourable complex with Eu(III) than the more highly charged tetra-substituted 3'pyridine species. Interestingly, the tetra-substituted 3'pyridine pendant arm system, **3**, forms more stable complexes than DOTAM which has simple amide pendant donor arms.⁴⁴ This increase in stability may be associated with the increasing hydrophobicity of the system. The larger aromatic structure of the pyridine groups compared with simple amides may interfere with the competitive complexing ability of water for the metal ion. This may be either as a consequence of increased steric hindrance to the approach of water to the complex or a change in water structure around the complex through an increase in hydrophobicity or both.⁴⁵

In addition to the ML formation constant a number of $\log K_a$'s for each metal ion complex were also identified; these are designated as M(LH) and ML(OH). The M(LH) species are as expected due to the early formation of the Eu(III) metal ion complex in solution for both ligands **3** and **4**. This is evidenced by the early departure from the pH titration curve of the ligand in the absence of Eu(III) ions.

Four M(LH) species were identified for ligand **3**, while only three M(LH) species were identified for ligand **4**. It can be anticipated that the vast majority of the M(LH) species identified for both ligands **3** and **4** may be associated with the deprotonation of the nitrogen of the pyridine group due to their similarity with the $\log K_a$ values observed for the free ligand. The strength of the proton-donor interaction of groups not in close proximity to the metal ion should only be slightly altered in the absence and presence of metal ion. Hence, the $\log K_a$ values associated with these sites are only expected to be slightly altered upon metal ion complexation as the pyridine groups are not involved in metal ion complexation. It is well known though that the electron withdrawing nature of the Eu(III) can reduce the pK_a of the amide group adjacent to the cyclen macrocyclic ring favouring loss of the amide proton. This event has been noted to

occur over the pK_a range of 6.5-8.^{46, 47} Therefore, assignment of these species is inconclusive due to the nature of the Eu(III) ion and the affect it has on surrounding functional groups.

Deprotonation of only one metal bound water molecule was observed for the Eu(III) complex of ligand **3**. In contrast deprotonation of two metal bound water molecules were observed for the Eu(III) complexes of ligand **4**. It is believed that the metal hydroxide complexes were formed from the coordination of water to the ML complex to give the conjugate acid ML(OH)_2 . Interestingly, the pH range over which deprotonation of the metal bound water molecule(s) for the Eu(III) complexes of ligands **3** and **4** was found to be quite similar. This suggests that ligand environment is more important than the number of coordinating ligand donor sites in determining the $\log K_a$ of the metal bound water molecules. Each Eu(III) ion complex was found to form a ML(OH) species in close approximation to the important physiological pH range of \sim pH 7.4. This suggests that the Eu(III) complex of **4** may show enhanced hydrolytic activity closer to physiological pH conditions compared with the corresponding La(III) complex. It is worth noting that the **3.Eu(III)** complex is known to be pH independent,³¹ however, it is anticipated that with two metal bound water molecules **4.Eu(III)** will be pH dependent.

In contrast to the formation of complexes with Eu(III) ions for both ligands **3** and **4** which formed at a very early pH, the La(III) complexes were not observed to form significantly until approximately pH 7. This can be clearly seen on Figure 2, where the dashed line for the pH titration in the presence of La(III) ions mirrors that of the pH titration of the ligand in the absence of metal until approximately pH 7. This suggests that both ligands form either very weak interactions with the La(III) ions or that formation is kinetically very slow. Above pH 7 though the pH titration curves for both ligands **3** and **4** in the presence of La(III) ions does depart from the titration curve of the ligand alone. Unfortunately, this pH coincides with the formation of insoluble metal hydroxide species, which limits the available data set. The structure of the pH titration curves of both ligands **3** and **4** in the presence of La(III) ions was reproducible between pH 7-9 even when the concentration of La(III) ion used was varied. This suggests that the species giving rise to the

curves are associated with the ligand and not just the formation of the metal hydroxide species in solution. However, the precise determination of formation constants or $\log K_a$ values for the deprotonation of metal bound water molecules for the La(III) ion complexes with ligands **3** and **4** was not viable. However, the data suggests that the formation constants for the ML species of ligands **3** and **4** with La(III) are of the order of 10^6 - 10^7 . These are quite low compared with the Eu(III) ion complexes of ligands **3** and **4**. This can be ascribed to the relative sizes of the macrocyclic cavity and the metal ion and the lower surface charge density of the La(III) ion. A $\log K_a$ for the deprotonation of the metal bound water molecule(s) for the La(III) ion complexes with both ligands **3** and **4** can also be alluded to; $\log K_a \sim 8.6$. This again suggests that the pH at which the metal bound water molecule(s) is deprotonated is independent of the level of substitution of the macrocyclic ring. However, it must be again noted that the constants for the La(III) series were determined on a limited data set and are only indicative of the true values. The data used for the Eu(III) ion complexes is significantly larger and meets all the criteria for confidence required for the program used.⁴² The $\log K_a$ value for the deprotonation of the metal bound water molecule for La(III) ion complexes is different to that of the Eu(III) ion complexes. This reduction in $\log K_a$ values for ML(OH) can be ascribed to the fact that as the ionic radius of the lanthanide(III) decreases, the Lewis acidity of the metal ion increases and therefore lowers the $\log K_a$ value of the metal bound water molecules.

Overall the coordination ability of the lanthanide(III) ion has little effect on the deprotonation of the metal hydroxide complex. It is the surrounding ligand environment and the charge density of the lanthanide(III) ion that seems to control the $\log K_a$ of the metal bound water molecules. This information can be used to further design macrocyclic complexes of high stability with metal hydroxide $\log K_a$ values finely tuned for hydrolytic activity.

Rate of hydrolysis

The RNA mimic, 2-hydroxypropyl *p*-nitrophenyl phosphate (HPNP), was used in order to evaluate the efficiency of the metal ion complexes synthesised herein. The rate constants for the hydrolysis of HPNP by the metal ion complexes, **4.Ln(III)**, **5.Ln(III)**, **6.Ln(III)** and **7.Ln(III)** (Table 3), were determined by measuring the changes in absorption of the HPNP band at $\lambda = 300$ nm compared with the cleavage product (*p*-nitrophenolate) at $\lambda = 400$ nm.¹ The experimental conditions used were designed to mimic physiological conditions (pH 7.4 and 37 °C), which is important for the development of a ribonuclease mimics. The HEPES buffer (at 50 mM) was chosen due to its optimal pH range ($\log K_a$ value of HEPES is 7.55) while the high concentration was found to reduce pH drift of ± 0.2 pH units.⁴⁸ The most efficient complexes at promoting hydrolysis of HPNP were **4.Eu(III)** and **4.La(III)**, the pH rate profile of both is shown in Figure 3.

It is evident from Table 3 that changing the hydration states of the Eu(III) 3'pyridine complexes greatly influences the rate of cleavage of HPNP, while for La(III) 3'pyridine complexes the rate enhancement is less effected.⁴⁹ The tri-substituted 3'pyridine complex, **4.Eu(III)**, is four times more efficient than the corresponding tetra-substituted species, **3.Eu(III)**. The extra coordination site in the tri-substituted 3'pyridine Eu(III) ion system, **4.Eu(III)**, probably enhances substrate binding and promotes hydrolysis. This is in agreement with the findings of Morrow and co-workers, who have shown that increased rate constants can be obtained when two metal bound water molecules are present.⁴⁸

The MLH species are as expected due to the early formation of the Eu(III) metal ion complex in solution for both ligands **3** and **4**.

This is evidenced by the early departure from the pH titration curve of the ligand in the absence of Eu(III) ions.

The pH-rate profile for the two La(III) 3'pyridine complexes, **3.La(III)** and **4.La(III)**, was similar regardless of the level of substitution (ESI Figure S5); both complexes exhibited a bell shaped curve maximum at around pH 8.4 for hydrolytic activity. The rate at pH 8.4 is three times higher than that measured at pH 7.4 for both complexes. The pH dependence of both these systems indicates that the reaction is catalysed by both acid and base and that the maximum rate constant is achieved when both are present. While the exact $\log K_a$ values for the La(III) complexes could not be determined potentiometrically a discussion based on trends is still valid and follows hence.

The enhanced rate at pH 8.4 corresponds to the formation of the ML(OH) species that was alluded to from the potentiometric titrations of ligands **3** and **4** in the presence of La(III). This supports previous research which has shown that the $\log K_a$ value of a metal bound water molecule gives a good indication of the pH-rate dependence exhibited by a system.^{50, 51} The decrease in the rate constant beyond pH 8.4 may be associated with the deprotonation of the second metal bound water molecule determined to be associated with both **3.La(III)** and **4.La(III)** through elemental analysis. A dihydroxy species is not expected to be able to bind the negatively charged phosphodiester, thus slowing down the hydrolysis upon formation.

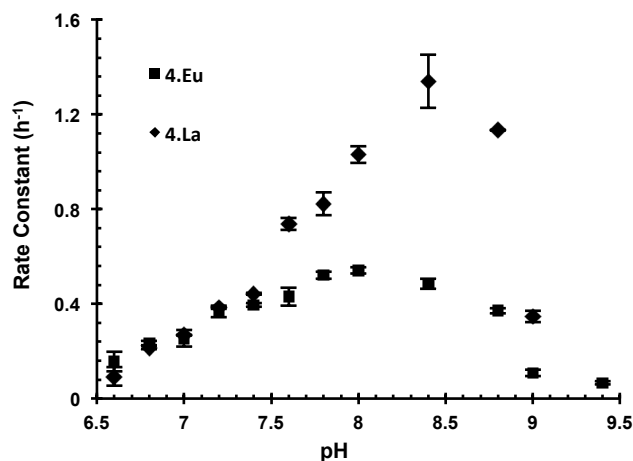


Fig. 3 The pH-rate profile for the hydrolysis of 0.14 mM HPNP at 37 °C by **4.Eu(III)** (0.18 mM) (square) and **4.La(III)** (0.18 mM) (diamond). Each data point is an average of 2-3 measurements, agreeing to within 15%. The error bars are determined from the average of the 2-3 measurements.

Analysis of the rate constant as a function of pH for the tri-substituted 3' pyridine Eu(III) derivative, **4.Eu(III)**, showed a bell shaped curve with a maximum around pH 8.0 (ESI Figure S3). This is at a lower pH value than that observed for the La(III) complex, **4.La(III)**. This is as expected, based on the $\log K_a$ values of the metal bound water molecules for **4.Eu(III)** (Table 2). This shift towards physiological pH ~ 7.4 in the optimal pH range for hydrolytic activity for the tri-substituted 3' pyridine Eu(III) complex system, **4.Eu(III)**, compared with the corresponding La(III) system, **4.La(III)**, is very important in the design of ribonuclease mimics. This can be accounted for by analysing the speciation diagrams for **4.Eu(III)** (ESI Figure S6), which clearly show that for **4.Eu(III)** both the ML(OH) and ML(OH)₂ species begin to form at a relatively low pH. However, the pH dependency of the rate profile for **4.Eu(III)** is in stark contrast to the pH profile observed for the

previously reported tetra substituted 3' pyridine complex, **3.Eu(III)**, where the rate of hydrolysis was independent of pH.³¹ This indicates that the two metal bound water molecules of the tri-substituted 3' pyridine Eu(III) complex, **4.Eu(III)**, play an important role in influencing the pH behaviour of the system.

This suggests that by 'fine-tuning' these systems that we can achieve maximum hydrolytic efficiency at an optimal pH value by altering the hydration state of the metal ion and the $\log K_a$ of metal bound water molecule(s). Interestingly though a comparison of the rate enhancements of both the Eu(III) and La(III) tri-substituted 3' pyridine systems, **4.Eu(III)** and **4.La(III)**, showed that the

hydrolytic activity of the larger La(III) ion is still more efficient than Eu(III) even when the hydration state is increased, regardless of pH. For example the tri-substituted 3' pyridine Eu(III) complex, **4.Eu(III)**, exhibits a maximum rate at pH 8.0 but at pH 8.4 it is still less than 50% active compared with the tri-substituted 3' pyridine La(III) complex, **4.La(III)**.

The hydrolytic activity of the pseudo dipeptide complexes (Table 3) is also shown to increase with the size of the lanthanide(III) ion. This is consistent with previously reported systems.^{28,29}

Table 3. Pseudo first order rate constants (k), half-lives (t) and relative rates (k_{rel}) for the cleavage of HPNP (0.14 mM) in 50 mM HEPES at pH 7.4 and 37 °C for complexes **1.Ln(III)**, **2.Ln(III)**, **3.Ln(III)**, **4.Ln(III)**, **5.Ln(III)**, **6.Ln(III)**, **7.Ln(III)** at a concentration of 0.18 mM; where Ln(III) = La(III) or Eu(III).

Previously reported rate constants				Rate constants presented herein			
Complex	k (h^{-1})	$t_{1/2}$ (h)	k_{rel}^\dagger	Complex	k (h^{-1})	$t_{1/2}$ (h)	k_{rel}^\dagger
1.La(III) ²⁸	0.292 (± 0.023)	2.92	1966 (± 191)	4.La(III)	0.412 (± 0.006)	1.67	3433 (± 50)
1.Eu(III) ²⁸	0.048 (± 0.003)	14.38	400 (± 25)	4.Eu(III)	0.395 (± 0.012)	1.74	3292 (± 100)
2.La(III) ²⁹	0.039 (± 0.002)	17.6	325 (± 17)	5.La(III)	0.116 (± 0.011)	5.92	971 (± 92)
2.Eu(III) ²⁹	0.092 (± 0.004)	7.7	752 (± 33)	5.Eu(III)	0.025 (± 0.005)	25.55	210 (± 42)
3.La(III) ³¹	0.440 (± 0.014)	1.57	3666 (± 116)	6.La(III)	0.143 (± 0.015)	4.83	1192 (± 125)
3.Eu(III) ³¹	0.091 (± 0.007)	7.62	758 (± 58)	6.Eu(III)	0.030 (± 0.009)	22.62	254 (± 75)
				7.La(III)	0.066 (± 0.011)	10.41	555 (± 92)
				7.Eu(III)	0.056 (± 0.008)	12.37	466 (± 67)

Interestingly, the 'GlyGly' amino amide derivative, **5.La(III)**, showed a decrease in hydrolytic activity compared to the rate enhancement observed for the previously reported 'GlyGly' amino ester complex, **1.La(III)**. At pH 7.4 and 37 °C, HPNP was cleaved with a half-life of 4.83 h⁻¹ by **5.La(III)** (k_{rel} of 1192), while a half-life of 2.92 h⁻¹ (k_{rel} of 1966) was found for **1.La(III)**.

This may be attributed to the increased hydrogen bonding of the amide function which may have affected the formation of the hydrophobic cavity. The more bulky ester may be vital in forming the hydrophobic cavity. Previous work has shown that significant increases in bulk e.g. methyl to benzyl ester resulted in increased activity, but smaller increases in bulk e.g. methyl to ethyl resulted in decreased hydrolytic activity.²⁹ The activity of the benzyl ester system indicates that the hydrophobic cavity plays an important role in the activity of these compounds. Therefore, the observed decrease in rate constant for the amino amide systems **6.Ln(III)** might be due to the change in hydrophobic cavity around the metal ion. The rate constant for **5.La(III)** was shown to be strongly dependent on pH, however, no bell shape curve is observed in the range pH 6.6- 9.6 (ESI Figure S7). The rate constant was found to increase almost linearly as the pH increased and at pH 9.5, $k = 0.477$ (± 0.017), which represents a half-life of 1.44 h a $k_{rel} = 3975$ was determined. This was not anticipated as the parent 'GlyGly' system, **1.La(III)**,²⁸ exhibited pH dependence on the rate constant. The reduced hydrophobicity of the system (amides are less hydrophobic than esters) may have resulted in an increase in overall basicity and an increase in the $\log K_a$ value of the metal bound water. This may explain why a bell shaped curve was not observed in the measured pH range 6.6 - 9.6. Measurement of the $\log K_a$ value for the MLOH species for **5.La(III)** was not feasible.

The rate constant for the hydrolysis of HPNP by the 'GlyAla' pseudo dipeptide complex, **7.Ln(III)**, was found to be $k = 0.066$ (± 0.011) h⁻¹, which is significantly less than that observed of **5.La(III)** ($k = 0.143$ (± 0.015) h⁻¹), Table 3. However, **6.La(III)** was found to be much more effective than the previously reported

corresponding methyl ester complex **2.La(III)**, with $k = 0.039$ (± 0.002) h⁻¹.²⁹ This suggests that the amino amide arms may have a role to play in fine tuning the hydrophobic cavity.

Interestingly though, when a methyl group is introduced adjacent to the metal ion through *N*-methylation, **7.La(III)**, the rate of HPNP cleavage decreases. At pH 7.4 and 37 °C, **7.La(III)** was found to cleave HPNP with a pseudo first order rate constant of 0.116 (± 0.011) h⁻¹, corresponding to a half-life of 5.92 h and a $k_{rel} = 971$. A number of possible factors could contribute to the decreased activity of **7.La(III)** compared with the systems reported in this article and previously. The addition of a methyl group adjacent to the metal ion may prevent the hydrophobic cavity from forming due to the increased steric bulk. The increased rigidity of the system upon introduction of the *N*-methyl group may reduce the substrate binding; tertiary amides are known to be very rigid. The amide adjacent to the metal ion may play a key role in substrate binding (e.g. through hydrogen bonding). All of which may contribute to the decreased hydrolytic activity of the **5.Ln(III)** complex. This suggests that the size and shape of the hydrophobic cavity is a key consideration in increasing hydrolytic activity and that the role of the additional methyl group and amino amide at a distance from the metal ion warrants further investigation.

Conclusions

In this contribution we synthesised a series of novel lanthanide(III) ion complexes and investigated the role that lanthanide(III) ion, $\log K_a$, hydration state and hydrophobicity have on the hydrolysis of phosphodiester HPNP. Our results demonstrate that complexes involving the larger La(III) ion showed greater hydrolytic efficiency. Nevertheless, our results also show that complexes involving the smaller Eu(III) ion showed maximum activity at lower pH. For example the tri-substituted Eu(III) ion system with 3'-pyridine basic co-factors, **4.Ln(III)**, had a pH maximum close to pH 7.4, which is important for mimicking physiological conditions. Alteration of the

hydration state of the La(III) ion had little effect on the rate constant of HPNP cleavage, whereas alteration of the hydration state of the Eu(III) ion increased the observed rate constant for the hydrolysis of HPNP significantly. This further highlights the importance of having more than one free coordination site available for substrate binding.⁴⁸ Hydrolytic efficiency was found to be very sensitive to small changes in hydrophobicity and hydrogen bonding capabilities within the cavity. Our results suggest that the presence of a group capable of forming hydrogen bonds adjacent to the metal ion is key for hydrolysis. The information gained through this systematic investigation will be used in the further optimisation of dinuclear systems.

Experimental

Materials

Starting materials were obtained from Sigma Aldrich, Strem Chemicals and Fluka. Solvents used were HPLC grade unless otherwise stated. ¹H NMR spectra were recorded at 400 MHz using a Bruker Spectrospin DPX-400, with chemical shifts expressed in parts per million (ppm or *d*) downfield from the standard. ¹³C{¹H} decoupled NMR were recorded at 100 MHz using a Bruker Spectrospin DPX-400 instrument. Infrared spectra were recorded on a Mattson Genesis II FTIR spectrophotometer equipped with a Gateway 2000 4DX2-66 workstation. Mass spectroscopy was carried out using HPLC grade solvents. Mass spectra were determined by detection using Electrospray on a Micromass LCT spectrometer, using a Water's 9360 to pump solvent. The system was controlled by MassLynx 3.5 on a Compaq Deskpro workstation.

Synthesis

Synthesis of 2-Chloro-*N*-pyridin-3-yl-acetamide (**8**)⁵², (2-{4,7,10-Tris-[(methoxycarbonylmethyl-carbamoyl)-methyl]-1,4,7,10-tetraaza-cyclododec-1-yl}-acetyl-amino)-acetic acid methyl ester (**1**)²⁸ and 2-(2-{4,7,10-Tris-[(1-carbamoyl-ethylcarbamoyl)-methyl]-1,4,7,10-tetraaza-cyclododec-1-yl}-acetyl-amino)-acetic acid methyl ester (**2**)²⁹ were synthesized according to literature procedures and characterised by ¹H NMR. All mass spectrometry was performed in a 50/50 MeOH/H₂O solution. Note: trace Na was present in this solution.

Preparation of ligands 4, 5, 6 and 7

2-[4,7-Bis-(pyridin-3-ylcarbamolmethyl)-1,4,7,10-tetraaza-cyclododec-1-yl]-*N*-pyridin-3-yl-acetamide (4). Cyclen (0.48 g, 2.8 mmol), Cs₂CO₃ (2.738 g, 84 mmol) and KI (1.394 g, 84 mmol) were dissolved in 100 mL of dry MeOH. The mixture was stirred quickly and compound **8** (1.75 g, 84 mmol) was added in one addition. The resulting pale yellow solution was heated at 65 °C, under argon for 3 days. Upon cooling the inorganic salts were removed by filtration and the solvent was removed under reduced pressure. The product was purified by alumina column chromatography (TLC alumina 10% MeOH:90%DCM R_f 0.3) using gradient elution from 100% CH₂Cl₂ to 60% CH₂Cl₂:40% MeOH (with dissolved ammonia gas) to give a creamy white hygroscopic solid (0.58 g, 36% yield). M.p. 95-98 °C; Calculated for C₂₉H₃₉N₁₀O₃: [(M+H) peak] *m/z* (ES⁺) = 575.3207, Found: 575.3195 (-2.0 ppm); δ_H (CD₃OD, 400 MHz) 8.62 (d, *J* = 2.0 Hz, 1H, CCHN), 8.49 (d, *J* = 2.0 Hz, 2H, 2 x CCHN), 8.14 (d, *J* = 5.0 Hz, 1H, NCHCH), 8.08 (d, *J* = 4.5 Hz, 2H, 2 x NCHCH), 8.06 (br s, 1H, CCHCH), 7.94 (d, *J* = 4.5 Hz, 2H, 2 x CCHCH), 7.24 (dd, *J* = 5.5 Hz, 3.5 Hz, 1H, CHCHCH), 6.96 (dd, *J* = 5.5 Hz, 3.5 Hz, 2H, 2 x CHCHCH), 3.50 (s, 4H, 2 x NCH₂CO), 3.39 (s, 2H, NCH₂CO), 3.20 (s, 4H, NCH₂CH₂CO), 2.99 (s, 4H, NCH₂CH₂N), 2.84 (s, 4H, NCH₂CH₂N), 2.70 (s, 4H, NCH₂CH₂N); δ_C

(CD₃OD, 100 MHz) 171.4 (C=O), 170.4 (C=O), 143.4 (Ar), 143.1 (Ar), 140.0 (Ar), 139.5 (Ar), 135.5 (Ar), 135.1 (Ar), 127.2 (Ar), 126.8 (Ar), 124.3(Ar), 123.3(Ar), 57.5 (CH₂CO), 56.4 (CH₂CO), 54.1 (CH₂N), 51.1 (CH₂N), 49.5 (CH₂N), 44.7 (CH₂N); *m/z* (ES⁺) 575.3 (M+H)⁺, 597.3 (M+Na)⁺; IR ν_{max}(cm⁻¹) 3244, 3171, 3049, 2828, 1685, 1617, 1550, 1483, 1420, 1284, 1202, 1117, 953, 807, 706.

[(2-Chloro-acetyl)-methyl-amino]-acetic acid methyl ester (9). Sacrosine methyl ester.HCl (2.0 g, 14.2 mmol) and NEt₃ (3.18 g, 22.1 mmol) were added to CH₂Cl₂ (30 mL) and cooled below 0 °C in an ice/acetone bath. To this, a solution of chloroacetyl chloride (2.26 g, 20.4 mmol) in CH₂Cl₂ (20 mL) was added drop wise over 1 h. The reaction was then stirred at room temperature for a further 24 h. The resulting brown solution was filtered through celite and the filtrate was washed with 0.1 M HCl (3 x 20 mL). The organic layer was dried over K₂CO₃ and the solvent was removed under reduced pressure to yield a dark brown viscous liquid (1.35 g, 54% yield). Calculated for C₆H₁₁NO₃Cl: [(M+H) peak] *m/z* (ES⁺) = 180.0427, Found: 180.0436 (+4.7 ppm); δ_H (CDCl₃, 400 MHz) 4.13 (d, *J* = 2.5 Hz, 2H, ClCH₂CO), 4.09 (d, *J* = 2.5 Hz, 2H, NCH₂CH₂), 3.69 (s, 3H, NCH₃), 3.11 (s, 3H, OCH₃); δ_C (CDCl₃, 100 MHz) 168.6 (C=O), 166.7 (C=O), 51.7 (CH₂N), 49.2 (CH₃O), 40.5 (CH₂Cl), 36.31 (CH₃N); *m/z* (ES⁺) 180.04 (M+H)⁺ (Cl³⁵), 182.0395 (Cl³⁷), 202.02 (M+Na)⁺.

[Methyl-(2-{4,7,10-tris[(methoxycarbonylmethyl-methyl-carbamoyl)-methyl]-1,4,7,10-tetraaza-cyclododec-1-yl}-acetyl)-amino]-acetic acid methyl ester (5). Compound **9** (1.05 g, 6.9 mmol), cyclen (0.286 g, 1.66 mmol), Cs₂CO₃ (2.23 g, 6.9 mmol) and KI (1.14g, 6.9 mmol) were dissolved in dry MeCN (20 mL) and the resulting solution heated at reflux under argon for 3 days. The yellow solution was then filtered to remove the inorganic salts and then the solvent reduced under pressure. The resulting oil was solubilised in CH₂Cl₂ (30 mL) and washed with water (2 x 15 mL) and then saturated KCl solution (2 x 15 mL). The organic layer was extracted and dried over K₂CO₃. The solvent was removed under reduced pressure to give a pale yellow hygroscopic solid (0.92 g, 75% yield). M.p. 130-133 °C; Calculated for C₃₂H₅₆N₈O₁₂.3CH₂Cl₂: C, 42.05; H, 6.25; N, 11.21, Found: C, 42.06; H, 5.95; N, 11.70; Calculated for C₃₂H₅₇N₈O₁₂: [M+H peak] *m/z* = 745.4096, Found: 745.4066 (-4.0 ppm); δ_H (DMSO-*d*₆, 400 MHz) 5.76 (s, CH₂ from CH₂Cl₂) 4.11 (br s, 8H, NCH₂CO) 3.71 (br s, 8H, NCH₂CH₂), 3.64 (br s, 12H, NCH₃), 3.34 (br s, 16H, NCH₂CH₂N), 2.93 (t, *J* = 2.5 Hz, 12H, OCH₃); δ_C (DMSO-*d*₆, 100 MHz) 171.0 (C=O), 169.1 (C=O), 54.8 (CH₂), 52.1 (CH₂), 51.5 (CH₃), 49.0 (CH₂), 35.6 (CH₃N); *m/z* 745.40 (M+H)⁺; IR ν_{max} (cm⁻¹) 3438, 2953, 1754, 1488, 1357, 1215, 1099, 1002, 900, 830, 715.

***N*-Carbamoylmethyl-2-{4,7,10-tris-[(carbamoylmethyl-carbamoyl)-methyl]-1,4,7,10-tetraaza-cyclododec-1-yl}-acetamide (6).** Ammonia gas was bubbled through a solution of ligand **1** (0.15 g, 0.22 mmol) in dry MeOH (20 mL) at 0 °C for 1 h. The reaction mixture was then left to stir for 12 h at room temperature. The solvent was concentrated under reduced pressure to ~ 5 mL and left to stand for 1 h. A creamy white precipitate formed which isolated by filtration to yield the desired product (0.127 g, 91% yield). M.p. 154-158 °C; Calculated for C₂₄H₄₄N₁₂O₈.Na: C, 44.23; H, 6.81; N, 25.79, Found: C, 44.67; H, 6.54; N, 25.93; Calculated for C₂₄H₄₅N₁₂O₈: [M+H peak] *m/z* (ES⁺) = 629.3483, Found: 629.3464 (-1.9 ppm); δ_H (DMSO-*d*₆, 400 MHz) 8.60 (br s, 4H, NH), 7.29 (br s, 4H, NH₂), 7.00 (br s, 4H, NH₂), 3.65 (s, 8H, NHCH₂CO), 3.02 (s, 8H, CH₂CO), 2.69 (s, 16H, NCH₂CH₂N); δ_C (DMSO-*d*₆, 100 MHz) 170.9 (C=O), 170.78 (C=O), 79.1 (CH₂), 58.1 (CH₂), 48.5 (CH₂);

m/z (ES^+) 629.2 ($\text{M}+\text{H}^+$), 651.3 ($\text{M}+\text{Na}^+$); IR $\nu_{\text{max}}(\text{cm}^{-1})$ 3473, 3406, 3200, 2831, 1662, 1543, 1387, 1308, 1235, 629, 558.

2-(2-{4,7,10-Tris-[(1-cabamoly-ethylcarbamoyl)-methyl]-1,4,7,10-tetraaza-cyclododec-1-yl}-acetyl amino)-propionamide (7). Ammonia gas was bubbled through a solution of L-alanine methyl ester ligand, **2**,⁵³ (0.103 g, 0.13 mmol) in dry methanol (20 mL) for 1 h at 0 °C. The reaction mixture was then left to stir for 12 h at room temperature. The solvent was concentrated under reduced pressure to ~ 5 mL and left to stand for 1 h. A creamy white precipitate formed which isolated by filtration to yield the desired product (83 mg, 93% yield). M.p. 183-186 °C; Calculated for $\text{C}_{28}\text{H}_{52}\text{N}_{12}\text{O}_8\cdot\text{H}_2\text{O}\cdot\text{Na}$: C, 46.34; H, 7.50; N, 23.16, Found: C, 46.77; H, 7.55; N, 22.90; Calculated for $\text{C}_{28}\text{H}_{52}\text{N}_{12}\text{O}_8$: $[\text{M}+\text{Na} \text{ peak}] m/z (\text{ES}^+) = 707.3929$, Found: 707.3932 (+0.3 ppm); δ_{H} (DMSO-*d*₆, 400 MHz) 7.90 (br s, 4H, NH), 7.36 (br s, 4H, NH₂), 7.00 (br s, 4H, NH₂), 4.19 (m, 4H, CH), 3.04 (s, 8H, CH₂), 2.69 (s, 16H, NCH₂CH₂N), 1.22 (d, 12H, *J* = 6.5 Hz, CH₃); δ_{C} (DMSO-*d*₆, 100 MHz) 174.4 (C=O) 174.1 (C=O), 58.8 (CH₂), 52.8 (CH₂), 47.6 (CH₂), 18.8 (CH₃); m/z (ES^+) 685 ($\text{M}+\text{H}^+$), 707 ($\text{M}+\text{Na}^+$), 723 ($\text{M}+\text{K}^+$). IR $\nu_{\text{max}}(\text{cm}^{-1})$ 3313, 2822, 1662, 1541, 1306, 1236, 1106, 610.

General procedure for synthesis of lanthanide(III) complexes using lanthanide(III) triflate salts. Lanthanide(III) complexes were prepared by heating at reflux, under inert atmosphere, the ligand with 1.1 molar equivalents of the appropriate lanthanide(III) triflate in MeOH (10 mL) for 16 h, unless otherwise stated. The complexes were isolated by precipitation in dry ether (100 mL) or CH₂Cl₂ (100 mL) and the precipitates collected by filtration. ¹H NMR spectra of lanthanide(III) complexes consisted of very broad signals and therefore were not fully characterised *i.e.* it was not possible to determine integration. The same properties prevent ¹³C{¹H} spectra from being obtained. For ¹H NMR spectra, spectral width was set at 100 ppm (*i.e.*, -100 to 100).

2-[4,7-Bis-(pyridin-3-ylcarbamolymethyl)-1,4,7,10-tetraaza-cyclododec-1-yl]-*N*-pyridin-3-yl-acetamide.La.3CF₃SO₃.3H₂O (4.La(III)). Complex **4.La(III)** was prepared using ligand **4** (70 mg, 0.12 mmol) and La(CF₃SO₃)₃ (78 mg, 0.124 mmol). A pale yellow hygroscopic solid was obtained (121 mg, 86% yield). M.p. 225-228 °C; Calculated for $\text{C}_{29}\text{H}_{38}\text{N}_{10}\text{O}_3\text{La}(\text{III})\cdot 3\text{CF}_3\text{SO}_3\cdot 3\text{H}_2\text{O}$: C, 31.64; H, 3.65; N, 11.53, Found: C, 32.10; H, 3.34; N, 11.25; δ_{H} (D₂O, 400 MHz) 8.60, 8.52, 8.45, 8.17, 8.13, 7.91, 7.85, 7.23, 7.14, 3.86, 3.67, 2.87, 2.69; m/z (ES^+) 431.08 ($\text{M}+\text{CF}_3\text{SO}_3$)²⁺; IR $\nu_{\text{max}}(\text{cm}^{-1})$ 3492, 3275, 1654, 1564, 1486, 1437, 1284, 1166, 1028, 962, 808, 638, 516.

2-[4,7-Bis-(pyridin-3-ylcarbamolymethyl)-1,4,7,10-tetraaza-cyclododec-1-yl]-*N*-pyridin-3-yl-acetamide.Eu.CF₃SO₃.4.Eu(III). Complex **4.Eu(III)** was prepared using ligand **4** (52 mg, 0.09 mmol) and Eu(CF₃SO₃)₃ (59 mg, 0.099 mmol). A white hygroscopic solid was obtained (85 mg, 80% yield). M.p. 194-197 °C; Calculated for $\text{C}_{29}\text{H}_{38}\text{N}_{10}\text{O}_3\text{Eu}\cdot\text{CF}_3\text{SO}_3$: $[(\text{M}+\text{CF}_3\text{SO}_3)^{2+} \text{ peak}] m/z (\text{ES}^+) = 876.1861$, Found: 876.1838 (Eu¹⁵¹) (-2.6 ppm); δ_{H} (D₂O, 400 MHz) 19.07, 9.39, 8.25, 7.06, 6.62, 3.40, 2.87, 1.04, -6.43, -7.69, -10.49, -14.90, -18.48, -19.19; m/z (ES^+) 438.09 ($\text{M}+\text{CF}_3\text{SO}_3$)²⁺; IR $\nu_{\text{max}}(\text{cm}^{-1})$ 3447, 1623, 1569, 1507, 1430, 1252, 1167, 1029, 965, 837, 639.

2-[4,7-Bis-(pyridin-3-ylcarbamolymethyl)-1,4,7,10-tetraaza-cyclododec-1-yl]-*N*-pyridin-3-yl-acetamide.Tb.(4.Tb(III)). Complex **4.Tb(III)** was prepared using ligand **4** (64 mg, 0.11 mmol) and Tb(CF₃SO₃)₃ (74 mg, 0.122 mmol). A pale yellow hygroscopic solid was obtained (113 mg, 87% yield). M.p. 208-210 °C; Calculated for $\text{C}_{29}\text{H}_{38}\text{N}_{10}\text{O}_3\text{Tb}\cdot\text{CF}_3\text{SO}_3$: $[(\text{M}+\text{CF}_3\text{SO}_3)^{2+} \text{ peak}] m/z =$

(ES^+) 882.1902, Found: 882.1938 (+4.1 ppm); δ_{H} (D₂O, 400 MHz) 54.97, 42.76, 27.75, 16.01, 7.96, -2.54, -15.94, -27.91, -38.37, -58.00, -75.02, -80.82, -113.26, -123.07; m/z (ES^+) 441.09 ($\text{M}+\text{CF}_3\text{SO}_3$)²⁺; IR $\nu_{\text{max}}(\text{cm}^{-1})$ 3455, 3091, 1625, 1568, 1485, 1440, 1279, 1166, 1029, 965, 809, 703, 638.

[Methyl-(2-{4,7,10-tris[(methoxycarbonylmethyl-methyl-carbamoyl)-methyl]-1,4,7,10-tetraaza-cyclododec-1-yl}-acetyl-amino)-acetic acid methyl ester.La.CF₃SO₃ (5.La(III)). Complex **5.La(III)** was prepared using ligand **5** (200 mg, 0.26 mmol) and La(CF₃SO₃)₃ (164 mg, 0.28 mmol). An orange/yellow solid was obtained (315 mg, 91% yield). M.p. 191-194 °C; Calculated for $\text{C}_{36}\text{H}_{64}\text{N}_8\text{O}_{12}\text{La}\cdot\text{CF}_3\text{SO}_3$: $[(\text{M}+\text{CF}_3\text{SO}_3)^{2+} \text{ peak}] m/z (\text{ES}^+) = 1032.2602$, Found: 1032.2592 (-0.9 ppm); δ_{H} (CD₃CN, 400 MHz) 4.27, 3.84, 3.73, 3.12, 1.96; m/z (ES^+) 1118.31 ($\text{M}+2\text{CF}_3\text{SO}_3$)⁺, 516.12 (M^{2+}); IR $\nu_{\text{max}}(\text{cm}^{-1})$ 3496, 1745, 1612, 1457, 1274, 1164, 1031, 833, 640.

[Methyl-(2-{4,7,10-tris[(methoxycarbonylmethyl-methyl-carbamoyl)-methyl]-1,4,7,10-tetraaza-cyclododec-1-yl}-acetyl-amino)-acetic acid methyl ester.Eu.CF₃SO₃ (5.Eu(III)). Complex **5.Eu(III)** was prepared using ligand **5** (150 mg, 0.21 mmol) and La(CF₃SO₃)₃ (132 mg, 0.22 mmol). A yellow solid was obtained (232 mg, 82% yield). M.p. decomposed above 185 °C; Calculated for $\text{C}_{32}\text{C}_{56}\text{N}_8\text{O}_{12}\text{Eu}\cdot 3\text{CF}_3\text{SO}_3\cdot 3\text{H}_2\text{O}\cdot\text{CH}_2\text{Cl}_2$: C, 29.16; H, 4.35; N, 7.56, Found: C, 29.12; H, 3.90; N, 7.60; Calculated for $\text{C}_{36}\text{H}_{64}\text{N}_8\text{O}_{12}\text{Eu}\cdot\text{CF}_3\text{SO}_3$: $[(\text{M}+\text{CF}_3\text{SO}_3)^{2+} \text{ peak}] m/z (\text{ES}^+) = 1046.2750$, Found: 1044.27 (Eu¹⁵¹) 1046.2720 (Eu¹⁵³) (-2.9 ppm); δ_{H} (CD₃OD, 400 MHz) 60.58, 28.86, 8.30, -3.09, -7.57, -10.25, -13.15; m/z (ES^+) 1193.29 ($\text{M}+2\text{CF}_3\text{SO}_3$)⁺, 523.13 (M^{2+}); IR $\nu_{\text{max}}(\text{cm}^{-1})$ 3496, 2960, 1745, 1613, 1511, 1439, 1275, 1161, 1030, 834, 639.

***N*-Carbamoylmethyl-2-{4,7,10-tris-[(carbamoylmethyl-carbamoyl)-methyl]-1,4,7,10-tetraaza-cyclododec-1-yl}-acetamide.La. (6.La(III)).** Complex **6.La(III)** was prepared using ligand **6** (74 mg, 0.117 mmol) and La(CF₃SO₃)₃ (76 mg, 0.129 mmol). A white solid was obtained (110 mg, 79% yield). M.p. decomposed above 150 °C; Calculated for $\text{C}_{24}\text{H}_{44}\text{N}_{12}\text{O}_8\text{La}$: $[(\text{M})^{3+} \text{ peak}] m/z (\text{ES}^+) = 767.2390$, Found: 767.2364 (La¹³⁸) 768.25 (La¹³⁹) (-3.4 ppm); δ_{H} (D₂O, 400 MHz) 8.98, 7.48, 6.94, 3.73, 3.31, 2.05; m/z (ES^+) 255.69 (M^{3+}), 382.9 (M^{2+}), 1064.8 ($\text{M}+2\text{CF}_3\text{SO}_3$)⁺; IR $\nu_{\text{max}}(\text{cm}^{-1})$ 3423, 3332, 1691, 1632, 1431, 1251, 1029, 971, 678.

***N*-Carbamoylmethyl-2-{4,7,10-tris-[(carbamoylmethyl-carbamoyl)-methyl]-1,4,7,10-tetraaza-cyclododec-1-yl}-acetamide.Eu. (6.Eu).** Complex **6.Eu** was prepared using ligand **6** (48 mg, 0.076 mmol) and Eu(CF₃SO₃)₃ (50 mg, 0.084 mmol). A white solid was obtained (59 mg, 63% yield). M.p. 224-228 °C; Calculated for $\text{C}_{24}\text{H}_{44}\text{N}_{12}\text{O}_8\text{Eu}$: $[(\text{M})^{3+} \text{ peak}] m/z (\text{ES}^+) = 780.2539$, Found: 779.26 (Eu¹⁵¹) 781.2571 (Eu¹⁵³) (+3.2 ppm); δ_{H} (D₂O, 400 MHz) 25.73, 6.63, 2.19, 1.12, -0.06, -1.82, -4.61, -7.12, -9.15, -12.68; m/z (ES^+) 390.21 (M^{2+}), 465.23 ($\text{M}+\text{CF}_3\text{SO}_3$)²⁺, 1079.12 ($\text{M}+2\text{CF}_3\text{SO}_3$)⁺; IR $\nu_{\text{max}}(\text{cm}^{-1})$ 3345, 1698, 1630, 1419, 1248, 1164, 1029, 972, 638, 573.

2-(2-{4,7,10-Tris-[(1-cabamoly-ethylcarbamoyl)-methyl]-1,4,7,10-tetraaza-cyclododec-1-yl}-acetyl amino)-propionamide.La. (7.La(III)). Complex **7.La(III)** was prepared using ligand **7** (48 mg, 0.067 mmol) and La(CF₃SO₃)₃ (43 mg, 0.074 mmol). A creamy/white solid was obtained (35 mg, 47% yield). M.p. 238-241 °C; Calculated for $\text{C}_{28}\text{H}_{52}\text{N}_{12}\text{O}_8\text{La}$: $[(\text{M}^{3+}) \text{ peak}] m/z = (\text{ES}^+) 822.3016$, Found: 823.3052 (La¹³⁸) 824.31 (La¹³⁹) (-3.6 ppm); δ_{H} (D₂O, 400 MHz) 4.60, 4.25, 3.00, 1.31; m/z (ES^+) 411.03 (M^{2+}), 486

(M+CF₃SO₃)²⁺, 1120.91 (M+2CF₃SO₃)⁺; IR ν_{\max} (cm⁻¹) 3287, 3241, 1685, 1626, 1458, 1250, 1167, 1063, 1029, 957, 640.

2-(2-{4,7,10-Tris-[(1-cabamoly-ethylcarbamoyl)-methyl]-1,4,7,10-tetraaza-cyclodec-1-yl}-acetyl amino)-propionamide.Eu.(7.Eu(III)). Complex **7.Eu(III)** was prepared using ligand **7** (20 mg, 0.029 mmol) and Eu(CF₃SO₃)₃ (19 mg, 0.037 mmol). A creamy white solid was obtained (29 mg, 78% yield). M.p. decomposed above 230 °C; Calculated for C₂₈H₅₂N₁₂O₈Eu: [(M³⁺) peak] m/z (ES⁺) = 837.3244, Found: 835.32 (Eu¹⁵¹) 837.3208 (Eu¹⁵³) (-3.6 ppm); δ_{H} (CD₃OCD₃, 400 MHz) 33.44, 26.63, 6.62, 4.39, 3.16, 0.36, -5.21, -7.6, -10.36, -13.26, -14.16; m/z (ES⁺) 278.3 (M)³⁺, 417.94 (M)²⁺, 1134.62 (M+2CF₃SO₃)⁺; IR ν_{\max} (cm⁻¹) 3327, 3261, 1689, 1629, 1443, 1248, 1165, 1043, 1029, 965, 638.

Potentiometric Titrations

Deionised water that had been purified with the MilliQ-Reagent system to produce water with a specific resistance of >15 M Ω cm⁻¹, boiled for 30 min to remove CO₂, and cooled under a drying tube filled with soda lime, was used in the preparation of all aqueous solutions. All metal salts were standardised in triplicate by means of a cation exchange chromatography. Potentiometric titrations were performed using an automatic titrator system, MOLSPIN, equipped with a glass electrode (Orion Ross Sureflow 8172 BN combination electrode) and connected to a Dell PC. The titrations were carried out at 25 °C in a water-jacketed vessel. Argon was bubbled firstly through a 1 M KOH solution and then through a solution of 0.1 M NEt₄ClO₄. The dry argon was then bubbled through the cell to exclude CO₂ and O₂. Milli-Q water and NEt₄ClO₄ were prepared as described as above. All solutions were prepared using 100% water, with constant ionic strength $I = 0.1$ M (NEt₄ClO₄). The protonation constants were determined by the titration of a 0.1 M NEt₄OH with a 10 cm³ solution of a ligand and HClO₄. The NEt₄OH was previously standardised against potassium hydrogen phthalate. The determination of metal complex ion stability constants for each ligand was carried out by the addition of one equivalent of the metal salt solution to the acidified titration solution. The stability constants for each metal complex ion were determined by means of the Fortran programme HYPERQUAD.⁴² The final constants represent an average from two calculated titrations where the chi-squared of each run was less than 12.6 at the 95% confidence level. Speciation diagrams were determined using the speciation program HySS.⁵⁴

Lifetime Determination for Eu(III) and Tb(III) Complexes

Luminescent lifetime measurements were carried out on Varian Carey Eclipse Fluorimeter for **4.Eu(III)** (λ_{ex} 395 nm, λ_{em} 615 nm) and **4.Tb(III)** (λ_{ex} 366 nm, λ_{em} 545 nm); delay time (0.1ms), gate time (0.01 ms), total decay (10ms). The pH/pD of each solution was adjusted to pH/pD 7.4 prior to measurement.

Kinetic evaluations

All kinetic evaluations were carried out using an Agilent 8453 spectrophotometer or a Varian CARY 50 spectrophotometer. The Agilent 8453 spectrophotometer was fitted with a circulating temperature controlled bath, and water driven mechanical stirring. The Varian CARY 50 spectrophotometer was fitted with a thermostatted block and a mechanical stirrer. The stirring rate of the mechanical stirrer in the Varian CARY 50 spectrophotometer was set to a similar rate to that of the Agilent 8453 spectrophotometer, following a series of kinetic measurements. The rate of hydrolysis (k) of the phosphodiester by the complexes prepared in Chapter 2 and Chapter 3 were determined by fitting the data to first order kinetics using *Biochemical Analysis Software* for Agilent ChemStation and Software version 3.00(182) for the CARY 50

spectrophotometer. All reactions gave 'pseudo'- first order kinetics, with errors of $\pm 15\%$. A 50 mM solution of HEPES was prepared (1.19 g) in deionised water (100 mL). The pH of the solution was adjusted to the desired pH using either 2 M NaOH solution or 2 M HCl solution. Using this buffer, a 0.14 mM solution of HPNP was prepared. The concentration was adjusted such that the Abs = 1.22 ($\epsilon = 6777$). 2.4 mL of this HPNP solution was then incubated in a quartz UV cell at 37 °C for 10 mins. This gave 4.2×10^{-7} mol of the phosphodiester. A solution of the appropriate lanthanide(III) complex was prepared in methanol such that a 100 μ L contained 4.32×10^{-7} mol of the complex (0.18 mM). A 100 μ L was then added to the HPNP solution at 37 °C and the reaction was monitored by UV over at least 16 h. The pH was checked at the end of some of the reactions and was found to have changed by no more than ± 0.05 pH units.

Acknowledgements

We thank Enterprise Ireland, IRCSET and TCD for financial support and Dr John E. O'Brien for assisting with NMR. We particularly thank COST CM1005 Supramolecular Chemistry in Water for financial support.

Notes and references

^a School of Chemistry and Trinity Biomedical Sciences Institute, University of Dublin, Trinity College Dublin, Dublin 2, Ireland. E-mail: gunnlaut@tcd.ie.

^b Sansom Institute, School of Pharmacy and Medical Sciences, University of South Australia, Adelaide, Australia. E-mail: Sally.Plush@unisa.edu.au.

[†] k_{rel} is the ratio between k and the rate constant of the uncatalysed reaction, which was measured to be 0.00012 h⁻¹, $\tau_{1/2} = 5.78 \times 10^3$ h, at pH 7.4

Electronic Supplementary Information (ESI) available: [Figures S1-7]. See DOI: 10.1039/b000000x/

1. R. Breslow and D. L. Huang, Proc. Nat. Acad. Sci. USA, 1991, 88, 4080.
2. N. H. Williams, B. Takasaki, M. Wall and J. Chin, Acc. Chem. Res., 1999, 32, 485.
3. M. W. Bowler, M. J. Cliff, J. P. Waltho and G. M. Balckburn, New J. Chem., 2010, 34, 784-794.
4. A. Radzicka and R. Wolfenden, Science, 1995, 267, 90.
5. A. Streedhara and J. A. Cowan, J. Biol. Inorg. Chem., 2001, 10, 337-347.
6. M. Zhao, H.-B. Wang, L.-N. Ji and Z.-W. Mao, Chem. Soc. Rev., 2013, 42, 8360.
7. F. Mancin, P. Scrimin, P. Tecilla and U. Tonellato, Chem. Commun., 2005, 2540.
8. F. Mancin, P. Scrimin and P. Tecilla, Chem. Commun., 2012, 48, 5545.
9. S. C. L. Kamerlin, P. K. Sharma, R. B. Prasad and A. Q. Warshel, Rev. Biophys., 2013, 46, 1.
10. D. Desbouis, I. P. Troitsky, M. Belousoff, L. Spicca and B. Graham, Coord. Chem. Rev., 2012, 256, 897.
11. H. Lonnberg, Org. Biomol. Chem., 2011, 9, 1687.
12. F. Mancin and P. Tecilla, in *Metal Complex-DNA interactions*, ed. N. Hadjilias and E. Sletten, John Wiley & Sons, Ltd, Chichester, UK2009.
13. L. Tjioe, T. Joshi, J. Brugger, B. Graham and L. Spicca, Inorg. Chem., 2011, 50, 621-635.
14. M. A. Camargo, A. Neves, A. J. Bortoluzzi, B. Szpoganicz, F. L. Fischer, H. A. Terenzi, O. A. Serra, V. G. Santos, B. G. Vaz and M. N. Eberlin, Inorg. Chem., 2010, 49, 6013-6025.
15. K. Nwe, C. M. Andolina and J. R. Morrow, J. Am. Chem. Soc., 2008, 130, 14861-14871.
16. A. M. Fanning, S. E. Plush and T. Gunnlaugsson, Chem. Commun., 2006, 3791-3793.

17. A. Roigk, O. V. Yescheulova, Y. V. Fedorov, O. A. Fedorova, S. P. Gromov and H. J. Schneider, *Org. Lett.*, 1999, 1, 833-835.
18. J. R. Morrow, R. L. Amyes and J. P. Richard, *Acc. Chem. Res.*, 2008, 41, 539.
19. J. R. Morrow and O. Iranzo, *Curr. Opin. Chem. Biol.*, 2004, 8, 192-200.
20. K. E. Sifers, S. A. Sander and J. R. Morrow, in *Progress in Inorganic Chemistry*, ed. K. D. Karlin, John Wiley & Sons Inc, Hoboken, New Jersey 2014, vol. 59.
21. J. R. Morrow, *Comments Inorg. Chem.*, 2008, 29, 169-188.
22. J. R. Morrow, in *Metal Ions in Biological Systems*, ed. A. Sigel and H. Sigel, Marcel Dekker, New York 1996, vol. 33, p. 561.
23. T. Gunnlaugsson, D. F. Broughman, A. M. Fanning, M. Nieuwenhuyzen, J. E. O'Brien and R. Viguier, *Org. Lett.*, 2004, 6, 4805-4808.
24. U. Baykal and E. U. Akkaya, *Tetrahedron Lett.*, 1998, 39, 5861.
25. M. Belousoff, P. Ung, C. M. Forsyth, Y. Tor, L. Spicca and B. Graham, *J. Am. Chem. Soc.*, 2009, 131, 1106-1114.
26. S. J. Franklin, *Curr. Opin. Chem. Biol.*, 2001, 5, 201-208.
27. M. J. Wiester, P. A. Ulmann and C. A. Mirkin, *Angew. Chem. Int. Ed.*, 2011, 50, 114-137.
28. T. Gunnlaugsson, R. J. H. Davies, M. Nieuwenhuyzen, C. S. Stevenson, R. Viguier and S. Mulready, *Chem. Commun.*, 2002, 2136.
29. T. Gunnlaugsson, R. J. H. Davies, M. Nieuwenhuyzen, J. E. O'Brien, C. S. Stevenson and S. Mulready, *Polyhedron*, 2003, 22, 711.
30. T. Gunnlaugsson, J. E. O'Brien and S. Mulready, *Tetrahedron Lett.*, 2002, 43, 8493.
31. T. Gunnlaugsson, R. J. H. Davies, P. E. Kruger, P. Jensen, T. McCabe, S. Mulready, J. E. O'Brien, C. S. Stevenson and A. M. Fanning, *Tetrahedron Lett.*, 2005, 46, 3761-3766.
32. W. D. Horrocks and D. R. Sudnick, *Acc. Chem. Res.*, 1981, 14, 384.
33. A. Beeby, I. M. Clarkson, R. S. Dickens, S. Faulkner, D. Parker, A. S. Royal, A. S. de Sousa, J. A. G. Williams and M. Woods, *J. Chem. Soc., Perkin Trans. 2*, 1999, 493.
34. H. Korhonen, T. Koivusalo, S. Toivola and S. Mikkola, *Org. Biomol. Chem.*, 2013, 11, 8324-8339.
35. C. I. Maxwell, N. J. Mosey and R. S. Brown, *J. Am. Chem. Soc.*, 2013, 135, 17209.
36. X. Zhang, Y. Zhu, H. Gao and C. Zhao, *Inorg. Chem.*, 2014.
37. S. Aime, M. Botta and G. Ermondi, *Inorg. Chem.*, 1992, 31, 4291.
38. P. Caravan, J. J. Ellison, T. J. McMurry and R. B. Lauffer, *Chem. Rev.*, 1999, 99, 2293.
39. A. Ahmed, R. A. Bragg, J. Clayden, L. W. Lai, C. McCarty, J. H. Pink, N. Westlund and S. A. Yasin, *Tetrahedron*, 1998, 54, 13277.
40. V. M. Shelton and J. R. Morrow, *Inorg. Chem.*, 1991, 31, 4295.
41. A. Bencini, A. Bianchi, E. Garcia-Espana, M. Micheloni and J. A. Ramirez, *Coord. Chem. Rev.*, 1999, 188, 97.
42. P. Gans, A. Sabatini and A. Vacca, *Talanta*, 1996, 43, 1739.
43. M. Braddock, D. Fox and D. Rotella, *Biomedical Imaging: The Chemistry of Labels, Probes and Contrast Agents*, Royal Society of Chemistry, Cambridge 2011.
44. A. Pasha, G. Tircsó, E. T. Benyó, E. Brücher and A. D. Sherry, *Eur. J. Inorg. Chem.*, 2007, 4340.
45. S. E. Plush, S. F. Lincoln and K. P. Wainwright, *Dalton Trans.*, 2004, 9, 1410-1417.
46. C. McCoy, F. Stomeo, S. E. Plush and T. Gunnlaugsson, *Chem. Mater*, 2006, 18, 4336.
47. S. E. Plush, N. A. Clear, J. P. Leonard, A. M. Fanning and T. Gunnlaugsson, *Dalton Trans.*, 2010, 39.
48. S. Amin, J. R. Morrow, C. H. Lake and M. R. Churchill, *Angew. Chem. Int. Ed. Engl.*, 1994, 33, 773.
49. A. Shahid, D. A. Voss Jr, W. D. Horrocks, C. H. Lake, M. R. Churchill and J. R. Morrow, *Inorg. Chem.*, 1995, 34, 3294.
50. G. Feng, J. C. Mareque-Rivas, R. R. Torres Martin de Rosales and N. Williams, *J. Am. Chem. Soc.*, 2005, 127, 13470.
51. E. Kövái and R. Kramer, *J. Am. Chem. Soc.*, 1996, 118, 12704.
52. A. E. Adel Rahman, H. A. El-Sherif and A. M. Mahmoud, *Indian. Chem. Soc.*, 1981, 58, 171.
53. S. Mulready, PhD, University of Dublin, Trinity College, 2004.
54. L. Alderighi, P. Gans, A. Ienco, D. Peters, A. Sabatini and A. Vacca, *Coord. Chem. Rev.*, 1999, 184, 311.